

Restricted feedback control of one-dimensional maps

Kevin Hall^{1,*} and David J. Christini^{2,†}

¹ *Entelos, Inc., Menlo Park, CA 94025*

² *Division of Cardiology, Department of Medicine,*

Weill Medical College of Cornell University, New York, NY 10021

(February 9, 2020)

Abstract

Dynamical control of biological systems is often restricted by the practical constraint of unidirectional parameter perturbations. We show that such a restriction introduces surprising complexity to the stability of one-dimensional map systems and can actually improve controllability. We present experimental cardiac control results that support these analyses. Finally, we develop new control algorithms that exploit the structure of the restricted-control stability zones to automatically adapt the control feedback parameter and thereby achieve improved robustness to noise and drifting system parameters.

PACS numbers: 05.45.Gg, 07.05.Dz, 87.17.Nn, 87.19.Hh

Typeset using REV_TE_X

*email: hall@entelos.com

†email: dchristi@med.cornell.edu

I. INTRODUCTION

Recent success controlling complex dynamics of nonlinear physical and chemical systems [1–16] has opened the door for the control of biological rhythms. Some researchers have speculated about the medical implications of controlling heart-rate dynamics or brain rhythms [17–22]. However, biological systems typically have characteristics that require special consideration. For example, biological control studies to date [17,23,18,24–26,21,27–30] have required that the control interventions be unidirectional — only allowing shortening of a parameter. Such a restriction is somewhat analogous to trying to balance a broomstick vertically on one’s palm using horizontal hand movements in only one direction. Intuitively, one might expect that such a restriction would limit controllability. However, as we will demonstrate in this paper, such a restriction introduces some surprising complexity to the stability properties of controlled one-dimensional map systems.

In fact, the unidirectional restriction can actually improve the controllability of some systems [31]. In this paper, we will show how restricted control can introduce stability zones that do not exist in the unrestricted case. Furthermore, we will show that some of these zones were present in recent cardiac control experiments [21]. Finally, we will exploit the structure of the stability zones in robust new control algorithms that automatically adapt the control feedback parameter.

II. DELAYED FEEDBACK CONTROL OF SYSTEMS DESCRIBED BY ONE-DIMENSIONAL MAPS

In this study we will consider the control of systems whose dynamics can be described by one-dimensional maps:

$$X_{n+1} = f(X_n, \lambda), \quad (1)$$

where X_n is the variable to be controlled and λ is an experimentally accessible system parameter. The goal is to stabilize the system state point $\xi_n = [X_n, X_{n-1}]$ about an unstable period-1 fixed point $\xi^* = [X^*, X^*]$, where $X^* = f(X^*, \lambda)$, by perturbing λ by an amount:

$$\delta\lambda_n = \frac{\alpha}{2}(X_{n-1} - X_n), \quad (2)$$

where α is the feedback gain parameter.

The advantage of such a control scheme is that relatively little *a priori* system information is required to implement control and stabilize ξ^* . The only requirement is knowledge of the sign of $\frac{\partial f}{\partial \lambda}$ so that perturbations can be applied in the correct direction. In fact, knowledge of the value of ξ^* is unnecessary because the controlled system's fixed point is identical to that of the uncontrolled system. Furthermore, if the fixed point drifts during the course of the control (as is common for biological systems), the controlled system will track the fixed point, provided that the system stays in the stable range of the feedback gain parameter α .

The control algorithm of Eq. 2 is an example of delayed feedback control, a technique that has been used in a variety of modeling and experimental studies [2–4,32,10,24]. In section IV we will present an example of a biological system with constraints that restrict the control algorithm — only allowing unidirectional perturbations of λ . The purpose of this study is to examine the implications of such a restriction.

A. Linear stability analysis of unrestricted delayed feedback control

For unrestricted control, in which $\delta\lambda_n$ can be positive or negative, linearizing the controlled system about a fixed point at the origin gives:

$$\begin{aligned} X_{n+1} &= AX_n + \beta(Y_n - X_n), \\ Y_{n+1} &= X_n, \end{aligned} \quad (3)$$

where $A \equiv \frac{\partial f}{\partial X}|_{\xi^*}$ and $\beta \equiv \frac{\alpha}{2}(\frac{\partial f}{\partial \lambda})|_{\xi^*}$.

The eigenvalues of Eq. 3 are $(A - \beta \pm \sqrt{(A - \beta)^2 + 4\beta})/2$. The fixed point is stable provided that both eigenvalues fall inside the unit circle. This condition is met when:

$$-1 < \beta < \frac{1}{2}(A + 1), \quad (4)$$

for $A < 1$ [21,33]. Note that the stability zone shrinks to zero for $A \leq -3$, thereby limiting the applicability of the unrestricted control algorithm to maps with a sufficiently shallow slope (i.e., $-3 \leq A < 1$) at ξ^* . Furthermore, for $A > 1$ there exists no real value for β such that the eigenvalues fall within the unit circle. Thus, unstable positively-sloped fixed points cannot be stabilized.

III. RESTRICTED DELAYED FEEDBACK CONTROL

Restricting the above control algorithm by only allowing shortening of λ gives the following controller:

$$\delta\lambda_n = \Theta_n \frac{\alpha}{2} (X_{n-1} - X_n), \quad (5)$$

where

$$\Theta_n = \begin{cases} 1 & \text{if } (X_n - Y_n) > 0, \\ 0 & \text{otherwise.} \end{cases} \quad (6)$$

Thus, when $\Theta_n = 1$ the control is active (i.e., a perturbation is delivered), and when $\Theta_n = 0$ the control is inactive (i.e., no perturbation is given).

A. Linear stability analysis of restricted delayed feedback control

The restricted control algorithm of Eq. 5 gives the following linearized controlled system:

$$\begin{aligned} X_{n+1} &= AX_n + \Theta_n \beta (Y_n - X_n), \\ Y_{n+1} &= X_n. \end{aligned} \quad (7)$$

Geometrically, the restriction of Eq. 6 means that perturbations will only be applied if the state point ξ_n lies above the return-map line of identity $X_{n+1} = X_n$. The dynamical effects of this restriction depend on the sign of the slope at ξ^* .

1. Restricted control for $A < -1$

Typical dynamics of restricted control for negatively-sloped unstable directions ($A < -1$) are depicted in Fig 1. This figure shows eight control trials of a linear map with $A = -4$ for different values of β ; there are four examples of stable control and four examples of unstable control.

Figure 1(a) shows a case in which the restricted control algorithm failed to stabilize the unstable fixed point ξ^* [which is located at the intersection of the uncontrolled system map (solid line) and the line of identity (dotted line), and is denoted by a solid triangle] with $\beta = -2.80$. The dot-dash lines correspond to the system maps when λ is perturbed. A series of arrows originate at the initial state point and connect consecutive state points (solid circles, numbered consecutively). In this case, the initial state point (1) is followed by a control intervention, which causes the next iterate (2) to fall below the line of identity. According to Eq. 6, the next iterate (3) will be uncontrolled and therefore will fall on the solid line. Furthermore, because the first controlled iterate (2) was less than the fixed point, the next iterate (3) will be above the line of identity, leading to a control intervention at the fourth iterate (4). Thus, control is applied every other iterate so that the sequence of Θ_n is 0101.... In this case, the fixed point is not stabilized because control fails to direct the system closer to the fixed point (i.e., the arrows spiral away from ξ^*).

Figure 1(b) shows control with the same value of A , but using a slightly more negative β value, $\beta = -3.1$. For these parameter settings, it can be seen that control is also applied every other iterate so that the sequence of Θ_n is again 0101.... However in this case, the fixed point is stabilized successfully because the control interventions direct the system closer to the fixed point (i.e., the arrows spiral towards ξ^*). Note that in order to maximize the clarity of the control sequence diagram, the axes in panel (a) are not scaled the same as those for panel (b). Similarly, for all of Fig. 1, axes from different panels are not necessarily scaled the same.

Figure 1(c) shows a trial in which β was decreased to -3.23 . As in the previous example, the first controlled iterate (3) is below the line of identity (dictating that the next iterate (4) is uncontrolled). However, in this case the perturbation is larger than would occur with the parameter settings of Fig. 1(b), such that the controlled iterate (3) is slightly larger than the fixed point. This

dictates that the next iterate (4) is below the line of identity, which leads to a second consecutive uncontrolled iterate (5). Thus, control is applied in a 001001... sequence. This sequence is stable for $\beta = -3.23$ because the control perturbations direct the system closer to the fixed point. However, if β is decreased to -3.40 , it can be seen from Fig. 1(d) that this generates a 001001... control sequence that is unstable because the system is directed away from the fixed point.

If β is made more negative, then a new control sequence is achieved. Figure 1(e) shows an unstable 011011... sequence for $\beta = -5.50$. In this case, the first perturbation is so large that the controlled iterate (2) is above the line of identity, dictating that the next iterate (3) is also controlled. The second controlled iterate (3) is below the line of identity and below the fixed point, thereby producing the 011011... sequence. In this case, the fixed point is not stabilized because the control perturbations moved the state point away from the fixed point. However, when β is decreased to -5.76 , as seen in Fig. 1(f), a 011011... sequence stabilizes the fixed point.

Like the transition from the stable 0101... sequence to the stable 001001... sequence depicted in Figs. 1(b) and (c), there is a transition from the stable 011011... sequence to the stable 00110011... sequence as β is decreased further. Figure 1(g) shows the stable 00110011... case for $\beta = -5.798$. The 00110011... sequence becomes unstable as β is decreased still further; Figure 1(h) depicts this case for $\beta = -5.95$.

The progression of unstable and stable periodic control sequences continues indefinitely as β is decreased. In fact, the switching parameter Θ_n imposes the following progression of control sequences as β is decreased from zero: unstable 01^1 , stable 01^1 , stable 001^1 , unstable 001^1 , unstable 01^2 , stable 01^2 , stable 001^2 , unstable 001^2 , ..., unstable 01^∞ , stable 01^∞ , stable 001^∞ , unstable 001^∞ , where 1^k denotes k consecutive ones (control perturbations) before the sequence repeats itself.

Because of the progression of the control sequences imposed by the switching term Θ_n , X_{k+1} can be expressed as:

$$X_{k+1} = e_k X_0, \quad (8)$$

where e_k is given by the following iterative expression:

$$e_k = (A - \beta)e_{k-1} + \beta e_{k-2}, \quad (9)$$

with $e_0 = A$ for all sequences and $e_1 = A^2 + \beta(1 - A)$ for the 01^k sequences or $e_1 = A^2$ for the 001^k sequences.

The boundaries of the stability zones can be computed by using the criterion that stable sequences move the system closer to the fixed point after one control sequence. Because X_{k+1} is the last iterate of the first 01^k control sequence and X_{k+2} is the last iterate of the first 001^k sequence, the stability conditions are $e_k < 1$ and $e_{k+1} < 1$ for the 01^k and 001^k sequences, respectively. Therefore, the boundaries are given by k degree polynomials in β . For example, the $k = 1$ control sequences are stable for $1 + A + 1/A \leq \beta \leq 1 + A$ for $A < -1$ [9]. Figure 2 depicts the stability zones (shaded regions) for $k = 1$ and $k = 2$. The boundaries between the stable 01^k and 001^k sequences are defined by the condition $e_k = 0$ (dotted curves in Fig. 2). These curves mark the optimal parameter values for a given stability region, because the fixed point is reached after a single control sequence 01^k .

The striking feature of this analysis is that the domain of control is extended by the restriction of Eq. 6 [31]. In fact, Fig. 2 shows that for all $A < -1$, stable control sequences exist for the restricted system. This is in contrast with the unrestricted system, for which stable control sequences exist only for $A > -3$, as shown by the dashed triangular region marking its stability zone (according to Eq. 4).

While there are an infinite number of stable zones corresponding to an arbitrary number k consecutive control perturbations, the stability zones are bounded by the curve $\beta = A - 2 - 2\sqrt{1 - A}$. This boundary is computed by recognizing that as k approaches infinity, control is always active and $X_{n+1} > X_n$ for every iterate. Thus, the algorithm behaves just like the unrestricted control of Eq. 3 with real eigenvalues greater than one — a condition met only when β is below the boundary.

2. Restricted control for $A > 1$

Typical dynamics of restricted control for positively-sloped unstable directions ($A > 1$) are depicted in Fig 3. This figure shows four control trials of a linear map, with $A = 2.1$, for different

values of β ; there are three examples of unstable control and one example where ξ^* is controlled.

Figure 3(a) shows an unstable 01^∞ sequence for $\beta = 1.5$. In this case, the perturbations are so small that all state points lie above the line of identity. The control slows the exponential growth (which would be marked by a rapid exit from ξ^* along the solid line), but fails to force an approach to ξ^* .

If β is decreased to $\beta = 2.5$, then the perturbations are large enough so that the first controlled X_n is smaller than the previous X_{n-1} . ξ_n then falls below the line of identity, thereby generating the 01^1 control sequence depicted in Fig. 3(b). In this case, the sequence is unstable because a given controlled point is further from ξ^* than the previous controlled point.

For $\beta = 3.5$, control is successful; the state point approaches ξ^* in a 01^1 sequence as shown in Fig. 3(c). Such control is successful for a noise-free model system. However, for a real-world system, once the state point is sufficiently close to ξ^* , noise will eventually kick ξ_n to the opposite side of ξ^* . Subsequent ξ_n will fall below the line of identity, causing the control to be deactivated and leading to an exponential departure from ξ^* .

When β is increased further, the first perturbation can be so large that the state point will be kicked to the other side of ξ^* as shown in Fig. 3(d) for $\beta = 4.5$. Again, control is subsequently deactivated and the system diverges from the fixed point.

The boundaries between the different control sequences are depicted in Fig. 4. The unstable 01^∞ sequence occurs for $\beta < A$. This boundary was computed by finding the value for β such that the first controlled iterate falls on the line of identity; this occurs for $\beta = A$. For $\beta > A$, the first controlled iterate lies below the line of identity, thereby shutting the control off for the next iterate. Thus, $\beta = A$ marks the boundary between the 01^∞ and 01^1 sequences. The boundary between unstable and stable 01^1 sequences was computed by finding the value for β such that the iterate subsequent to control is equal to the previous uncontrolled iterate; this occurs for $\beta = 1 + A$. For slightly larger β values, the iterate subsequent to control is closer to ξ^* than the previous uncontrolled iterate. Thus, the unstable 01^1 sequence is bounded by $A < \beta < 1 + A$. The final boundary marks the end of the converging 01^1 sequence and can be found by determining the value for β such that the first controlled iterate lands at ξ^* . This occurs for $\beta = A^2/(A - 1)$.

For $\beta > A^2/(A - 1)$, the first controlled iterate, and all subsequent iterates, lie below the line of identity thereby shutting of the control. Therefore, the converging 01^1 sequence occurs in the shaded region $1 + A < \beta < A^2/(A - 1)$ [9,34], and the unstable 010^∞ sequence occurs for $\beta > A^2/(A - 1)$.

Thus, for $A > 1$ the best that the restricted control algorithm can offer is a temporary reversal of divergence from the fixed point. However, in section V A we will make a simple modification to the restricted control algorithm for $A > 1$ that will keep the system in the vicinity of ξ^* in the presence of noise.

IV. EXPERIMENTAL OBSERVATION OF RESTRICTED CONTROL SEQUENCES

As described in Ref. [21], we have studied the control of a particular cardiac conduction interval, known as the atrioventricular (AV) nodal conduction time, in *in vitro* rabbit heart experiments. Because of the nonlinear excitation properties of AV-nodal tissue, the dynamics of AV-nodal conduction can bifurcate from a period-1 regime (where every impulse propagates through the AV-node at the same rate) to a period-2 regime (where propagation time alternates in a long, short, long, etc. pattern on a beat-to-beat basis) during rapid atrial excitation. It has been demonstrated [35,36] that these dynamics can be described by a period-doubling bifurcation of a one-dimensional map of the form of Eq. 1 where X_n is the AV-nodal conduction time and λ_n is the time between when the AV-node finishes conducting one impulse and when it starts conducting the next.

The goal in Ref. [21] was to eliminate the alternating rhythm by stabilizing the underlying period one fixed point X^* . This was achieved by delivering electrical stimuli to the atrial tissue in order to transiently shorten λ_n . Because there is no practical way to lengthen λ_n , the timing of the electrical stimuli was determined by the restricted controller of Eq. 5.

Although the *in vitro* rabbit cardiac system of Ref. [21] was not linear, application of the restricted control algorithm resulted in several of the control sequences predicted in the above linear system for $A < -1$. These control sequences were especially clear at the initiation of

control when perturbations were largest.

For example, Fig. 5(a) shows the variable X_n and the control parameter λ_n during an unstable 01^1 sequence for a feedback gain $\alpha = 3.3$ (corresponding to a negative β because $\frac{\partial f}{\partial \lambda} < 0$ in the cardiac control experiments). The first controlled beat is indicated by the arrow and corresponds to a negative perturbation of λ_0 (all control perturbations are negative as imposed by the switching term Θ_n). Because the system was nonlinear, oscillatory growth of X_n was quenched and the original large amplitude alternation of X_n was reduced in magnitude — but not eliminated.

When α was increased to 5.0 (as shown in Fig. 5(b); corresponding to a later segment of the same control trial that is shown in Fig. 5(a)), the system shifted to a stable 001^1 sequence that eliminated the alternation of X_n . After the fourth perturbation to λ_n (beat 303), the system shifted to a stable 01^1 sequence. This shift resulted from the close proximity of the 01^1 and 001^1 stable zones (Fig. 2); noise or drift in the system can cause such transitions.

Figure 5(c) shows a stable 001^2 control sequence that eliminated the alternation of X_n in a different rabbit heart using $\alpha = 2.5$. (Note that the α values from distinct trials are independent.) Similar to the sequence transitions in Fig. 5(b), the system switched to its adjacent stable 01^2 control sequence shortly after the control was initiated, and later switched back to the stable 001^2 control sequence.

V. MODIFICATIONS TO THE RESTRICTED CONTROL ALGORITHM

A. Automatic adaptation of the feedback gain for $A < -1$

Figure 5(a) (unsuccessful) and (b) (successful) demonstrate that successful control is dependent on the proper choice of α . Such dependence is a critical limitation given that the information required to determine the correct value of α (A , ξ^* , and $\frac{\partial f}{\partial X}|_{\xi^*}$) cannot be easily determined prior to control. Furthermore, the nonstationarities typical of biological systems imply that the appropriate value of α may drift over time, thereby increasing the likelihood of control failure if α is fixed. To eliminate the limitations of a fixed α value chosen prior to control, we have developed a new

technique that adaptively estimates α [37]. This adaptive approach is especially appropriate for applications (e.g., cardiac arrhythmia control) that cannot afford control failure of the type shown in the control attempt of Fig. 5(a).

This new technique exploits the structure of the stability zones to automatically adapt α such that ξ^* is stabilized more robustly. Because multiple perturbations away from the fixed point are not desirable, the optimal stability zone is the $k = 1$ zone. Furthermore, because the stable $k = 1$ zone has the largest area, it will be the most robust to noise and drifting system parameters. To target this zone, α is adapted according to:

$$\alpha_n = \begin{cases} \alpha_{n-1} + \delta\alpha & \text{if } \Theta_{n-4} \dots \Theta_{n-1} = 0101 \text{ or } 1010, \\ \alpha_{n-1} - \delta\alpha & \text{otherwise,} \end{cases} \quad (10)$$

where $\delta\alpha$ is a small increment. When $(\frac{\partial f}{\partial \lambda})|_{\xi^*}$ is negative (as in the cardiac experiments of Ref. [21]), α and $\delta\alpha$ are positive. Otherwise they are negative.

The algorithm of Eq. 10 is motivated by examining the stability zones in Fig. 2. For $k = 1$, optimal control occurs when β is at the boundary between stable 01^1 and stable 001^1 (dotted curve of Fig. 2). If β is too large, the control sequence will be 01^1 (unstable if β is so large that it is above the $k=1$ stability region or stable if β is within the stability region but above the optimal control boundary). In such a case, the adaptation of Eq. 10 will decrease β . In contrast, if β is too small, the control sequence will be 001^1 or some sequence with $k > 1$ (unstable if β is so small that it is below the $k = 1$ stability region or stable if β is within the stability region but below the optimal control boundary). In such a case, the adaptation of Eq. 10 will increase β . Thus, the adaptation will adjust the system so that it oscillates between the stable 01^1 and stable 001^1 sequences, provided that the increment $\delta\alpha$ is small enough so that the stepsize of β is sufficiently less than the height of the $k = 1$ stability zone. Specifically, the condition $|\delta\alpha| < |A(\frac{\partial f}{\partial \lambda})|_{\xi^*}|^{-1}$ ensures that the stepsize is less than half the height of the zone.

To illustrate the adaptive algorithm, we implemented the restricted controller of Eq. 5 with the feedback gain α replaced by α_n given by Eq. 10. α_0 was randomly chosen between -5 and -10 and $\delta\alpha = -0.1$. We applied this controller to the quadratic map:

$$X_{n+1} = \lambda_n X_n (1 - X_n) + \zeta_n, \quad (11)$$

where ζ_n is a normally-distributed random variable with a mean of zero and a variance of 0.001. The goal was to stabilize the fixed point $X^* = (\lambda_0 - 1)/\lambda_0$. Note that for the quadratic map, $(\frac{\partial f}{\partial \lambda})|_{\xi^*} = \frac{\lambda-1}{\lambda^2}$ is positive. Thus, the sign of the perturbations is opposite to that of the cardiac experiments of Ref. [21].

Figure 6 shows the results of an adaptive control trial of the quadratic map. For $1 \leq n \leq 500$, $\lambda_0 = 3.30$, corresponding to an uncontrolled stable period-2 orbit. Control was initiated at iterate $n = 125$ with an arbitrary initial value of $\alpha_n = -5.25$. The adaptive algorithm rapidly stabilized ξ^* as the adaptations of α_n kept the system in the $k = 1$ stability zone. The control was deactivated at $n = 375$ and the period-2 cycle returned.

At $n = 500$, λ_0 was switched to 3.52, which corresponds to a period-4 rhythm. Control was reactivated at $n = 625$ with an arbitrary initial value of $\alpha_n = -8.85$. The adaptive control stabilized ξ^* until the control was turned off at iterate 875. At $n = 1000$, λ_0 was switched to 3.65, which is in the chaotic regime. Control was reactivated at $n = 1125$ with an arbitrary initial value of $\alpha_n = -5.63$. ξ^* was stabilized after approximately 160 iterates. When control was deactivated at $n = 1375$ the chaos resumed. The oscillations in α_n , as governed by Eq. 10, are apparent in each control phase of the trial.

To demonstrate the ability of the adaptive algorithm to track a drifting fixed point, we applied the control algorithm to a quadratic map with $\lambda_0 = 3.0$ and λ_n increased by an increment of 0.001 every iterate ($\lambda_{n+1} = \lambda_n + 0.001$). As seen in Fig. 7, the small increments to λ_0 introduced a slow drift in the system dynamics and fixed point. Control was initiated at iterate 250 while the system was in its period-2 regime. Control was maintained for 500 iterates. During this period, X^* drifted from $X^* = 0.692$ to $X^* = 0.736$. Nevertheless, the control algorithm had no trouble tracking X^* . In fact, it can be seen that when control was deactivated at $n = 750$, the system had passed into the chaotic regime, an occurrence that did not disrupt control. However, if the feedback gain was held fixed rather than adapted, then control could not have been maintained for the entire control period (not shown).

B. Control of fixed points for $A > 1$

In section III A 2, we demonstrated that the restricted control algorithm can induce a transient approach towards ξ^* when $A > 1$. However, as mentioned, if the system is kicked to the other side of ξ^* , control is deactivated and the system diverges from ξ^* . If the algorithm could detect such an occurrence and reverse the sign of the perturbations, then ξ^* could be approached from the opposite side of ξ^* [38]. This idea motivates the following modification of the restricted control algorithm:

$$\delta\lambda_n = \hat{\Theta}_n \frac{\alpha_n}{2} (X_{n-1} - X_n), \quad (12)$$

where

$$\hat{\Theta}_n = \begin{cases} 1 & \text{if } \Phi_n(X_n - Y_n) > 0, \\ 0 & \text{otherwise,} \end{cases} \quad (13)$$

and

$$\Phi_n = \begin{cases} -1 & \text{if } \Theta_{n-4} \dots \Theta_{n-1} = 1000, \\ 1 & \text{otherwise.} \end{cases} \quad (14)$$

For stable control, a fixed value of the feedback gain ($\alpha_n = \alpha_0$) is chosen so that $1 + A < \beta < A^2/(A - 1)$. In order to adaptively control fixed points with $A > 1$, the controller in Eq. 12 can be used with a modified adaptive feedback gain algorithm:

$$\alpha_n = \begin{cases} \alpha_{n-1} + \delta\alpha & \text{if } \hat{\Theta}_{n-4} \dots \hat{\Theta}_{n-1} = 0101 \text{ or } 1010, \\ \alpha_{n-1} - \delta\alpha & \text{otherwise.} \end{cases} \quad (15)$$

Such a combination is feasible because the control-sequence boundaries for $A > 1$ dictate that Eq. 15 will direct the system towards the converging 0101... sequence (see Fig. 4). However, as in the case when $A < -1$, the increment in the feedback gain should be chosen such that α_n remains in the stable 0101... zone. Choosing $|\delta\alpha| < |(A - 1)(\frac{\partial f}{\partial \lambda})|_{\xi^*}|^{-1}$ ensures that the increment is less than half of the height of the zone.

In order to illustrate the control of an unstable fixed point with $A > 1$, we applied the modified control algorithm to the cubic map:

$$X_{n+1} = -4(m+1)X_n^3 + 6(m+1)X_n^2 - (2m+3)X_n + \lambda_n + \zeta_n, \quad (16)$$

where λ_n is perturbed according to Eq. 12 with $\lambda_0 = 1$, m is the slope of the map at the fixed point $X^* = 0.5$, and ζ_n is a normally-distributed random variable with a mean of zero and a variance of 0.001.

Figure 8 illustrates control of the cubic map without adaptation of the feedback gain (α_n is fixed at $\alpha_0 = 8.0$). For $1 \leq n \leq 500$, $m = 2.2$, corresponding to an uncontrolled stable period-2 orbit. After control was initiated at $n = 125$, X^* was stabilized after about 80 iterates. Stabilization of X^* was maintained until control was deactivated at $n = 375$, after which the system returned to the period-2 orbit. At $n = 500$, m was set to 2.7, which moved the system into the chaotic regime. Control was initiated at $n = 625$. After about 10 iterates, X^* was controlled for about 20 iterates. The system subsequently escaped control for about 30 iterates before control was recaptured and maintained until the algorithm was deactivated at $n = 875$.

The adaptive feedback gain algorithm is illustrated in Fig. 9, which shows control of a drifting cubic map with $m_{n+1} = m_n + 0.001$ and $m_0 = 2.0$. Control was activated for $250 < n < 750$. The fixed point was controlled successfully during this period. The fixed point location does not change for the drifting cubic map, but the system drifts into the chaotic regime by the end of the control period.

VI. CONCLUSION

Surprisingly, the typical biological restriction of unidirectional control perturbations enhances the controllability of fixed points with $A < -1$ in systems described by one-dimensional maps. Because biological systems typically drift over time, dynamic control algorithms must adapt to system nonstationarities. Although the restricted delayed feedback control technique allows for moderate tracking of the fixed point as long as the system remains within a stability zone, it is ill-suited for systems with significant drift. For such systems, automatic adaptation of the feedback

gain parameter ensures that the drifting system is directed to, and remains within, the largest stability zone. Thus, with the dual benefits of the increased stability of unidirectional restricted control and the adaptability of on-the-fly gain estimation, such control techniques could be of significant value to the control of biological systems. Indeed, a recent set of clinical experiments [39] have shown that adaptive restricted control of this type can successfully eliminate the same alternating AV-nodal conduction rhythm that was controlled in the rabbit experiments of Ref. [21]. Furthermore, we have shown that simple modifications of the restricted control algorithm can control fixed points with $A > 1$ — an impossible task for the unrestricted feedback controller. Thus, this algorithm may also have applicability in physical systems that allow bidirectional perturbations.

ACKNOWLEDGMENTS

This work was supported, in part, by a grant from the American Heart Association (0030028N) [DJC].

REFERENCES

- [1] W. L. Ditto, S. N. Rauseo, and M. L. Spano, *Physical Review Letters* **65**, 3211 (1990).
- [2] E. R. Hunt, *Physical Review Letters* **67**, 1953 (1991).
- [3] B. Peng, V. Petrov, and K. Showalter, *Journal of Physical Chemistry* **95**, 4957 (1991).
- [4] V. Petrov, B. Peng, and K. Showalter, *Journal of Chemical Physics* **96**, 7506 (1992).
- [5] R. Roy, T. W. Murphy, Jr., T. D. Maier, Z. Gills, and E. R. Hunt, *Physical Review Letters* **68**, 1259 (1992).
- [6] T. L. Carroll, I. Triandaf, I. Schwartz, and L. Pecora, *Physical Review A* **46**, 6189 (1992).
- [7] Z. Gills, C. Iwata, R. Roy, I. B. Schwartz, and I. Triandaf, *Physical Review Letters* **69**, 3169 (1992).
- [8] I. B. Schwartz and I. Triandaf, *Physical Review E* **48**, 718 (1993).
- [9] S. Bielawski, D. Derozier, and P. Glorieux, *Physical Review A* **47**, R2492 (1993).
- [10] D. J. Gauthier, D. W. Sukow, H. M. Concannon, and J. E. S. Socolar, *Physical Review E* **50**, 2343 (1994).
- [11] J. E. S. Socolar, D. W. Sukow, and D. J. Gauthier, *Physical Review E* **50**, 3245 (1994).
- [12] V. Petrov, M. J. Crowley, and K. Showalter, *Physical Review Letters* **72**, 2955 (1994).
- [13] N. F. Rulkov, L. S. Tsimring, and H. D. I. Abarbanel, *Physical Review E* **50**, 314 (1994).
- [14] P. Colet, R. Roy, and K. Wiesenfeld, *Physical Review E* **50**, 3453 (1994).
- [15] B. Hübinger, R. Doerner, W. Martienssen, W. Herdering, R. Pitka, and U. Dressler, *Physical Review E* **50**, 932 (1994).
- [16] D. J. Christini, J. J. Collins, and P. S. Linsay, *Physical Review E* **54**, 4824 (1996).
- [17] A. Garfinkel, M. L. Spano, W. L. Ditto, and J. N. Weiss, *Science* **257**, 1230 (1992).

- [18] S. J. Schiff, K. Jerger, D. H. Duong, T. Chang, M. L. Spano, and W. L. Ditto, *Nature* **370**, 615 (1994).
- [19] J. N. Weiss, A. Garfinkel, M. L. Spano, and W. L. Ditto, *Journal of Clinical Investigation* **93**, 1355 (1994).
- [20] L. Glass, *Physics Today* **49**, 40 (1996).
- [21] K. Hall, D. J. Christini, M. Tremblay, J. J. Collins, L. Glass, and J. Billette, *Physical Review Letters* **78**, 4518 (1997).
- [22] D. J. Christini, K. M. Stein, S. M. Markowitz, S. Mittal, D. J. Slotwiner, and B. B. Lerman, *Heart Disease* **1**, 190 (1999).
- [23] L. Glass and W. Zeng, *International Journal of Bifurcation and Chaos* **4**, 1061 (1994).
- [24] D. J. Christini and J. J. Collins, *Physical Review E* **53**, R49 (1996).
- [25] M. Watanabe and J. Robert F. Gilmour, *Journal of Mathematical Biology* **35**, 73 (1996).
- [26] M. E. Brandt and G. Chen, *International Journal of Bifurcation and Chaos* **6**, 715 (1996).
- [27] D. J. Christini and J. J. Collins, *CHAOS* **7**, 544 (1997).
- [28] M. E. Brandt, H.-T. Shih, and G. Chen, *Physical Review E* **56**, R1334 (1997).
- [29] T. Sauer, *Fields Institute Communication* **11**, 63 (1997).
- [30] D. J. Christini and D. T. Kaplan, *Physical Review E* **61**, 5149 (2000).
- [31] Independently discovered by Gauthier and Socolar using different techniques: D. J. Gauthier and J. E. S. Socolar, *Phys. Rev. Lett.* **79**, 4938 (1997).
- [32] K. Pyragas, *Physics Letters A* **170**, 421 (1992).
- [33] T. Ushio, *IEEE Transactions on Circuits and Systems-I* **43**, 815 (1996).
- [34] Bielawski *et al.* used an imposed 01^1 sequence in order to control unstable orbits of laser dy-

namics. Such a control scheme has the same 01^1 stability boundaries as our control algorithm with the exception that for $A > 1$ their imposed 01^1 control sequence is stable, rather than semi-stable as with our restricted control. The advantage of the approach proposed here is that the control sequence information can be used to automatically adapt the gain parameter.

- [35] J. Sun, F. Amellal, L. Glass, and J. Billette, *Journal of Theoretical Biology* **173**, 79 (1995).
- [36] F. Amellal, K. Hall, L. Glass, and J. Billette, *Journal of Cardiovascular Electrophysiology* **7**, 943 (1996).
- [37] Related techniques have been presented previously: G. W. Flake, G.-Z. Sun, Y.-C. Lee, and H.-H. Chen, in *Advances in Neural Information Processing*, edited by J. D. Cowan, G. Tesauro, and J. Alspector (Morgan Publishers, San Mateo, CA), 647 (1994); D. J. Christini and J. J. Collins, *IEEE Transactions on Circuits and Systems, I* **44**, 1027 (1997).
- [38] Note that this modification of the algorithm violates the biologically motivated restriction of unidirectional perturbations. Nevertheless, not all systems are subject to such restrictions.
- [39] D. J. Christini, K. M. Stein, S. M. Markowitz, S. Mittal, D. J. Slotwiner, M. A. Scheiner, S. Iwai, and B. B. Lerman, preprint (2000).

FIGURES

FIG. 1. Return maps showing the progression of control sequences as A is decreased below -1 . Sequential state points are numbered, the dotted diagonal line is the identity line $X_{n+1} = X_n$, the solid line is the map of the uncontrolled system with slope $A = -4$, the fixed point ξ^* is denoted by the solid triangle, and the dot-dash lines show the system map when perturbed by control interventions. (a) $\beta = -2.8$ results in an unstable 01^1 control sequence. (b) $\beta = -3.1$; stable 01^1 . (c) $\beta = -3.23$; stable 001^1 . (d) $\beta = -3.4$; unstable 001^1 . (e) $\beta = -5.5$; unstable 01^2 . (f) $\beta = -5.76$; stable 01^2 . (g) $\beta = -5.798$; stable 001^2 . (h) $\beta = -5.95$; unstable 001^2 . Note that axes from different panels are not necessarily scaled the same.

FIG. 2. Stability zones of unrestricted (Eq. 3) and restricted (Eq. 8) control for $A < -1$. The triangular region enclosed by the dashed lines in the upper right corner is the stability zone for unrestricted control. For restricted control, the $k = 1$ (01^1 and 001^1) and $k = 2$ (01^2 and 001^2) stability zones are the shaded regions enclosed by the solid curves (which are k -degree polynomials in β , determined via Eq. 9, as described in the text). The dotted curves inside the zones mark the transition from 01^k to 001^k . The annotated open circles **a–f** correspond to the control parameters for panels (a)–(f) of Fig. 1. The three vertically-spaced solid dots indicate that there are an infinite number of stability zones for larger k . The infinite sequence of stability zones is bounded by the curve $\beta = A - 2 - 2\sqrt{1 - A}$.

FIG. 3. Return maps showing the progression of control sequences as A is increased above 1. Sequential state points are numbered, the dotted diagonal line is the identity line $X_{n+1} = X_n$, the solid line is the map of the uncontrolled system with slope $A = 2.1$, the fixed point ξ^* is denoted by the solid triangle, and the dot-dash lines show the system map when perturbed by control interventions. (a) $\beta = 1.5$ results in an unstable 01^∞ control sequence. (b) $\beta = 2.5$; unstable 01^1 sequence. (c) $\beta = 3.5$; converging 01^1 sequence. (d) $\beta = 4.5$; unstable 010^∞ sequence. Note that axes from different panels are not necessarily scaled the same.

FIG. 4. Stability zones of restricted control (Eq. 8) for $A > 1$. The zone of semi-stability (shaded region; denoted 01^1) and the different zones of instability are separated by the curves $\beta = A$, $\beta = 1 + A$, and $\beta = A^2/(A - 1)$. The annotated open circles **a–d** correspond to the control parameters for panels (a)–(d) of Fig. 3.

FIG. 5. Control sequences observed in the rabbit heart experiments of Ref. [21]. The first control perturbation in each panel is indicated by an arrow. (a) An unstable 01^1 sequence for $\alpha = 3.3$. (b) The same preparation with $\alpha = 5.0$. In this case the control begins in a stable 001^1 sequence and shifts to a stable 01^1 sequence. (c) A stable 001^2 sequence, shifting to a stable 01^2 sequence, and returning to a stable 001^2 sequence in a different preparation with $\alpha = 2.5$.

FIG. 6. Adaptive control of the quadratic map of Eq. 11. Control was activated during the intervals labelled with a “C”. Iterates 125-375, 625-875, and 1125-1375 show control of period-2 ($\lambda_0 = 3.30$), period-4 ($\lambda_0 = 3.52$), and chaotic dynamics ($\lambda_0 = 3.65$), respectively.

FIG. 7. Adaptive control of a drifting quadratic map (Eq. 11). The baseline value of $\lambda_0 = 3.00$ was incremented by 0.001 each iterate ($\lambda_{n+1} = \lambda_n + 0.001$), causing a slow drift in the system. Control was activated from $250 \leq n \leq 750$ (labelled with a “C”). During this period, X^* drifted from $X^* = 0.692$ to $X^* = 0.736$. The adaptive algorithm tracked the drifting fixed point as the system moved into the chaotic regime.

FIG. 8. Control of the cubic map of Eq. 16 with $\lambda_0 = 1.0$. Control was activated during the intervals labelled with a “C”. Iterates 125-375 and 625-875 show control of period-2 ($m = 2.2$) and chaotic dynamics ($m = 2.7$), respectively.

FIG. 9. Adaptive control of a drifting cubic map (Eq. 16). The baseline value of $m_0 = 2.0$ was incremented by 0.001 each iterate ($m_{n+1} = m_n + 0.001$), causing a slow drift in the system. Control was activated from $250 \leq n \leq 750$ (labelled with a “C”). The fixed point location does not change for the drifting cubic map, but the system drifted into the chaotic regime by the end of the control period.

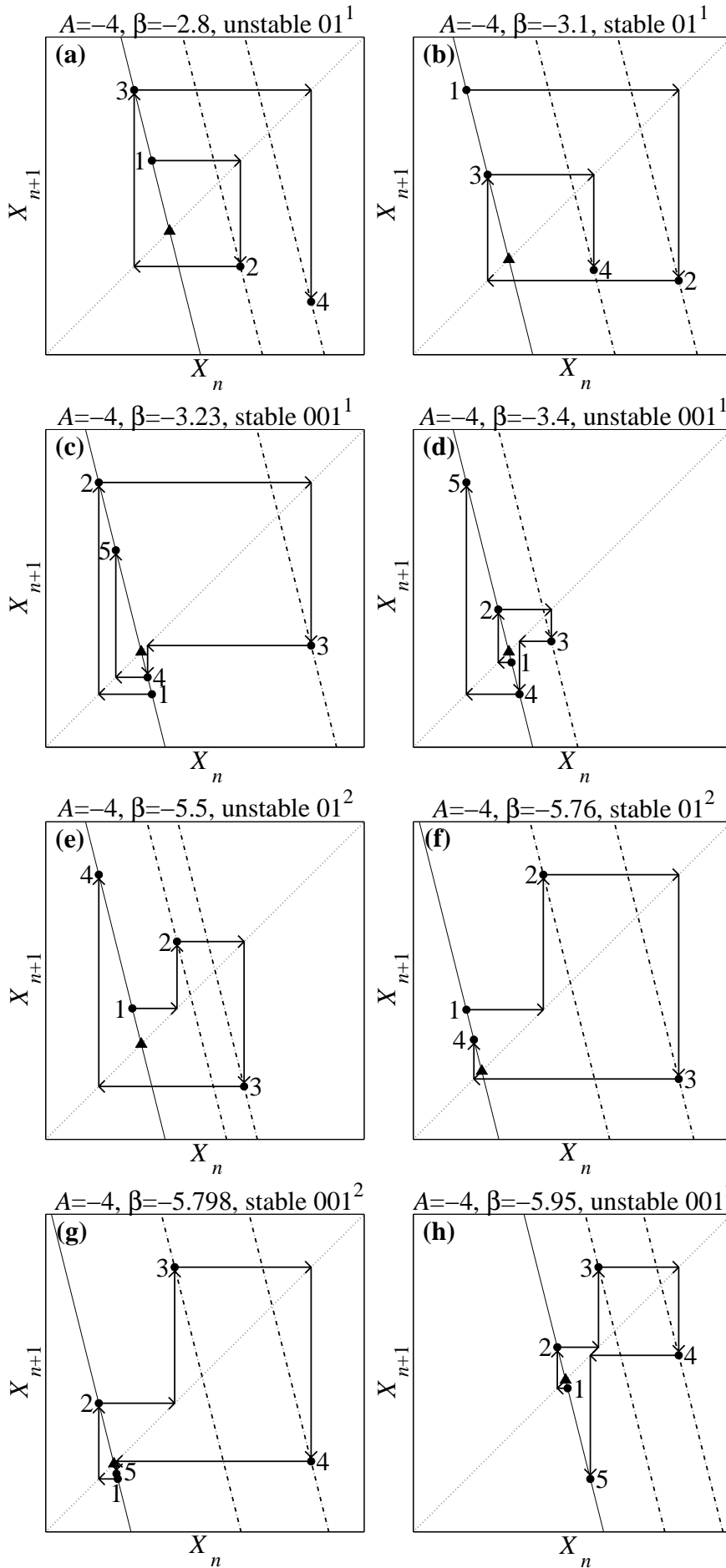


Fig. 1

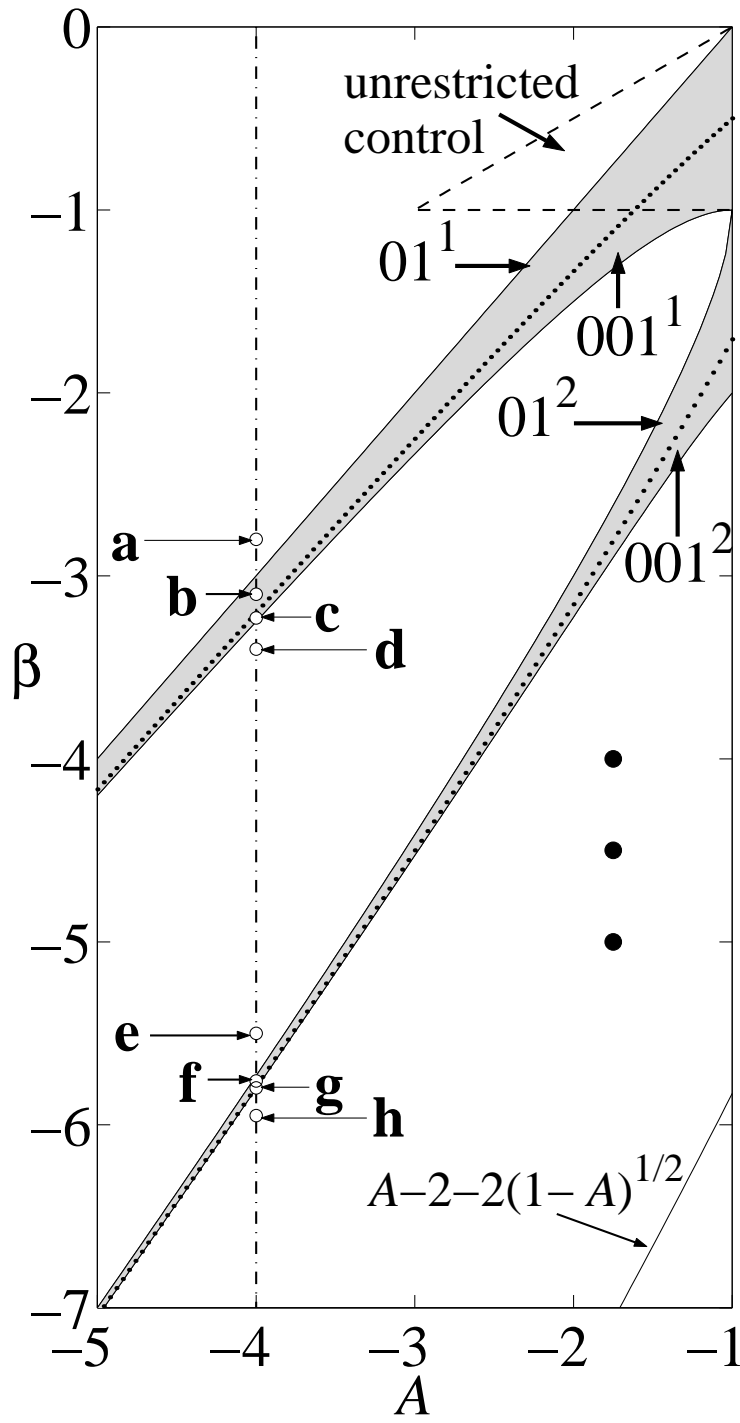


Fig. 2

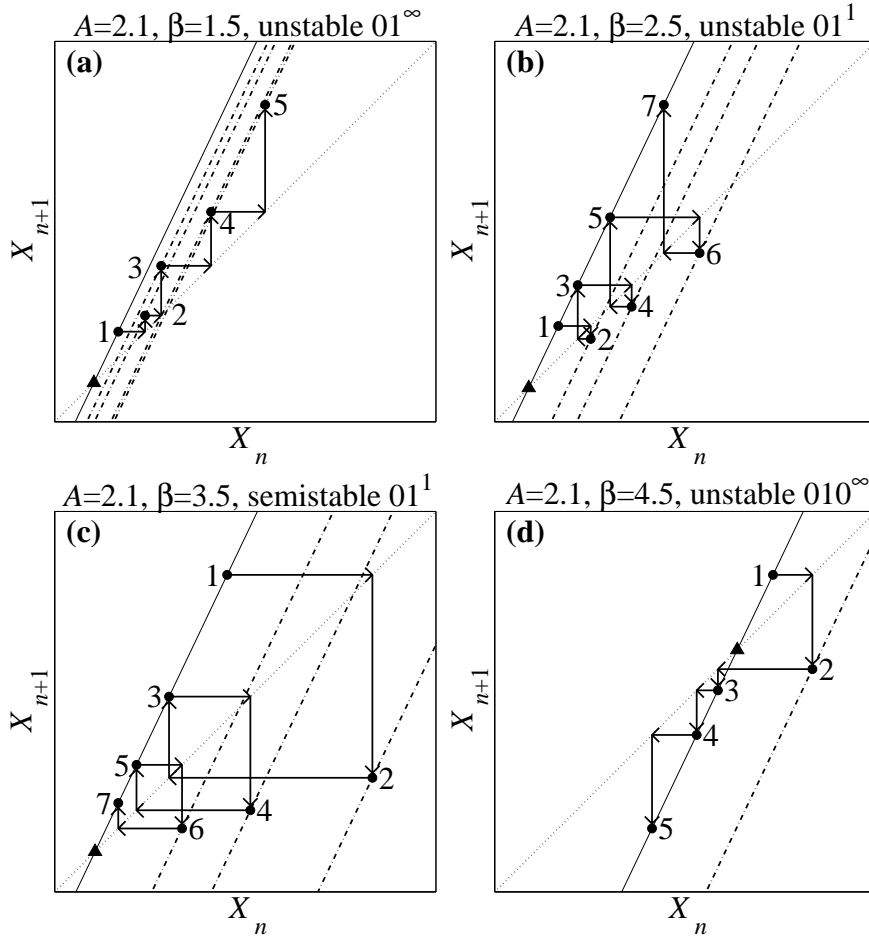


Fig. 3

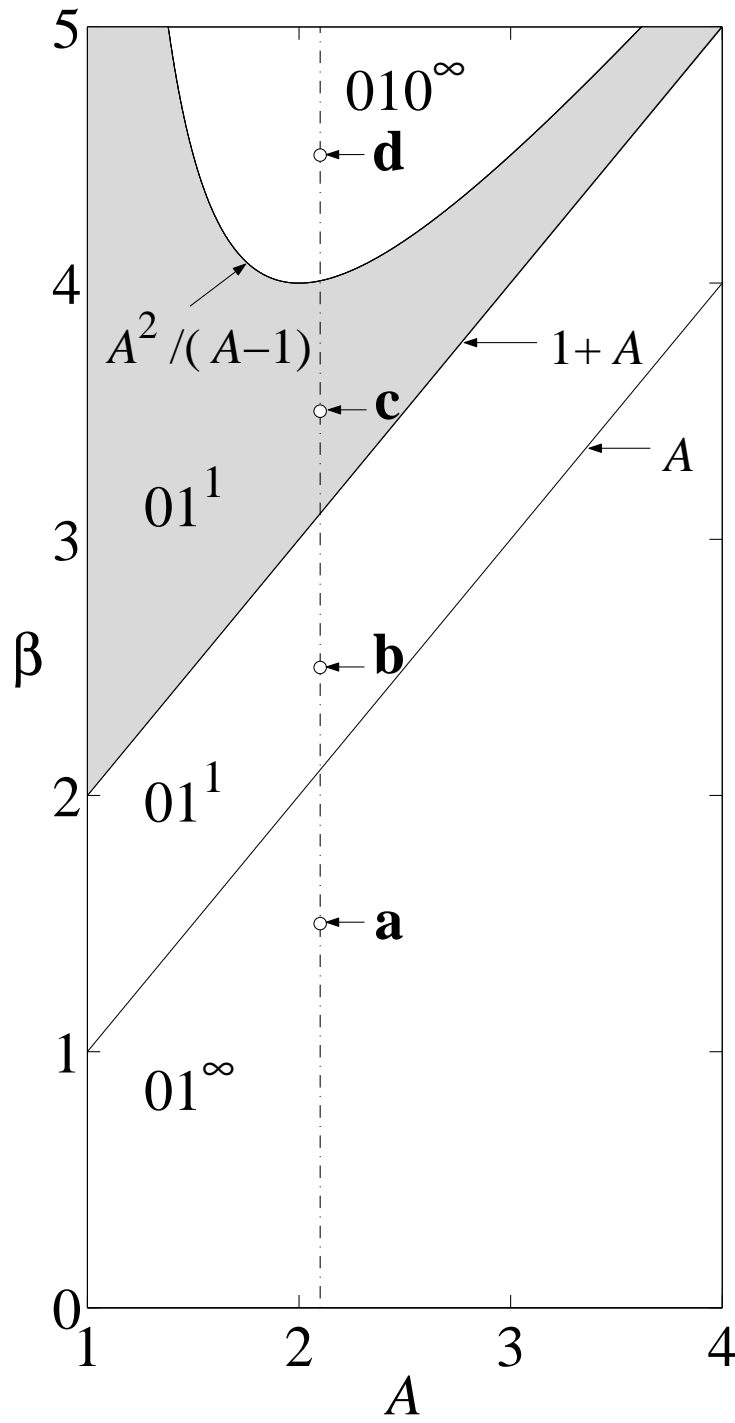


Fig. 4

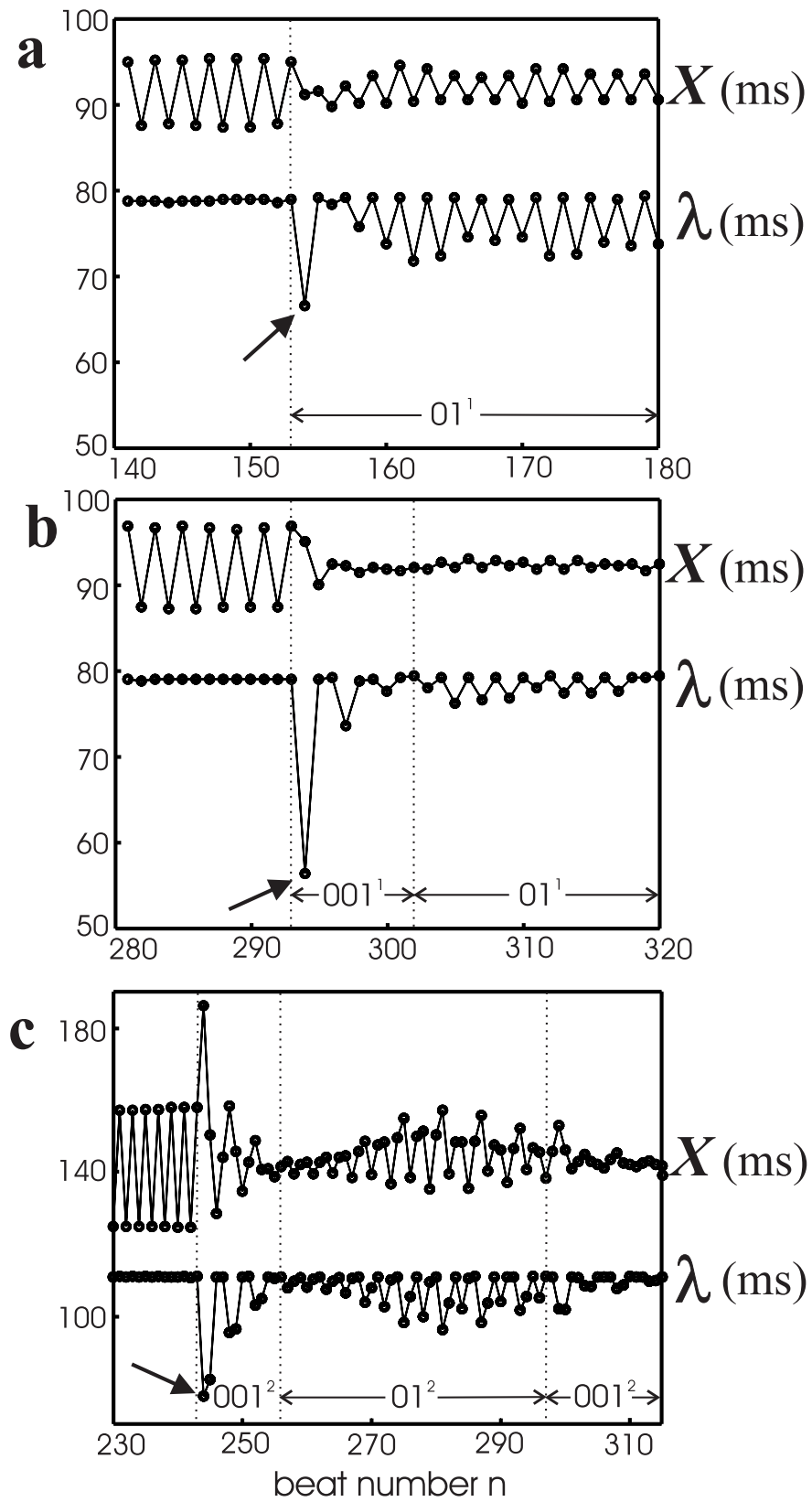


Fig. 5

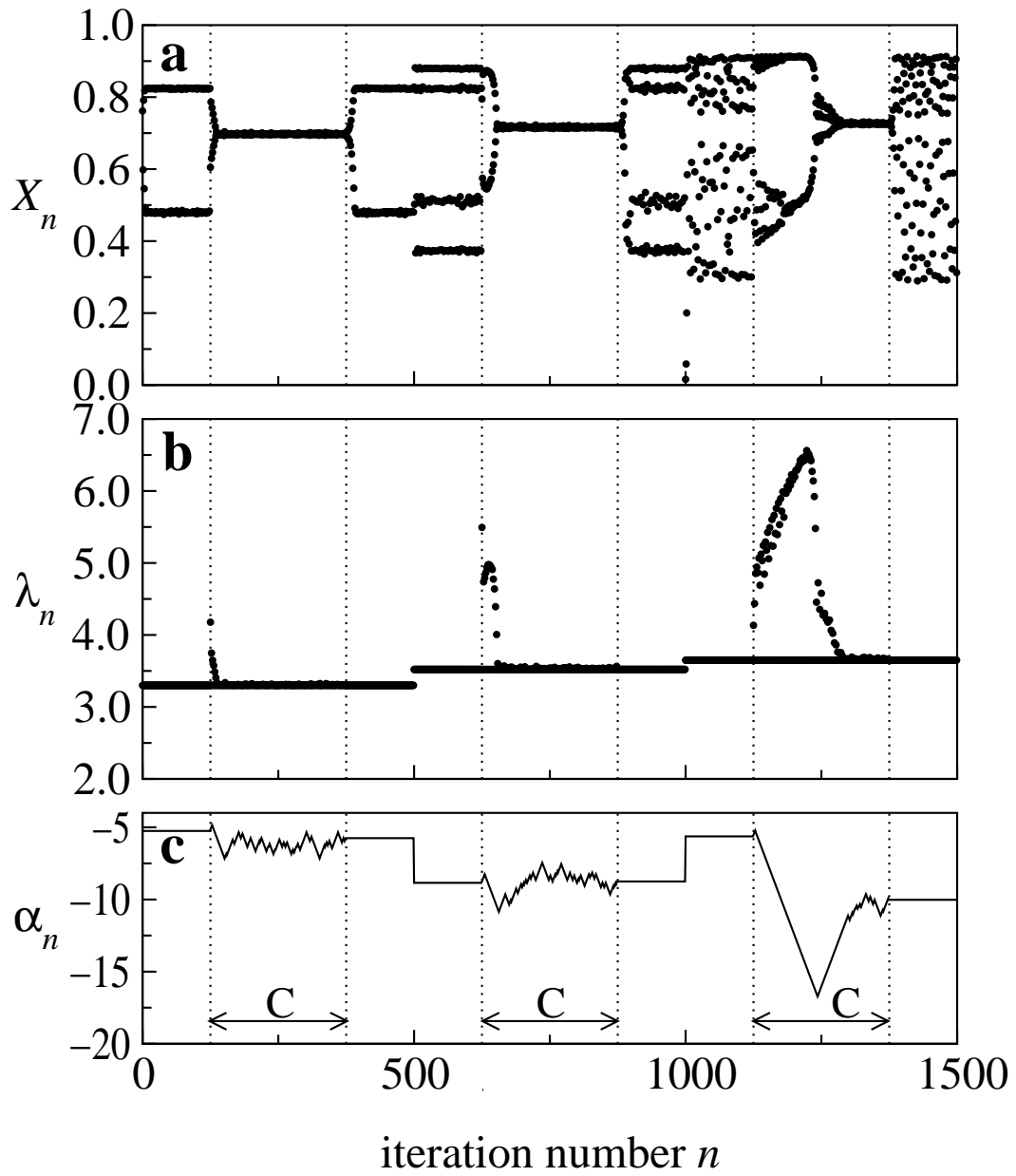


Fig. 6

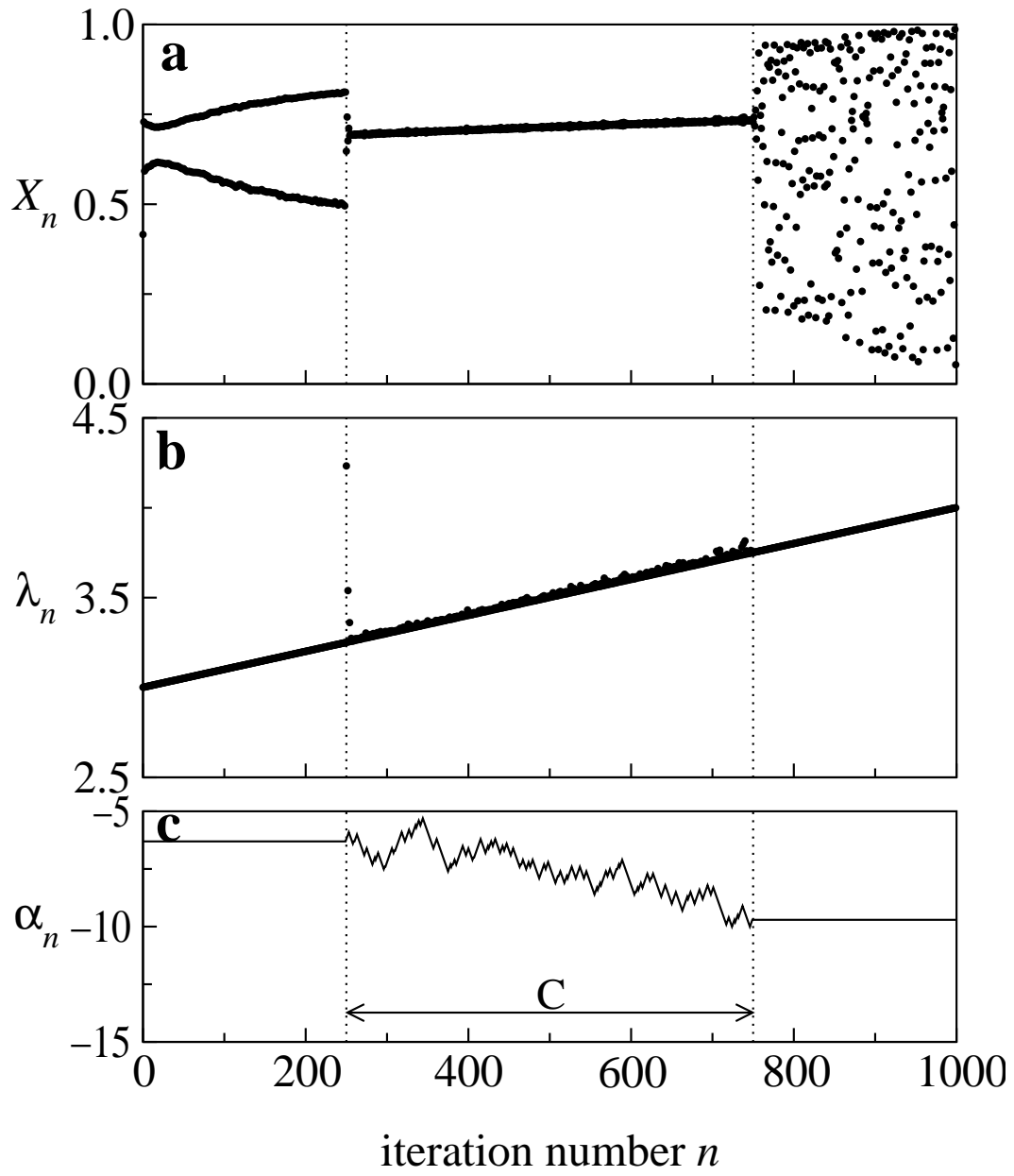


Fig. 7

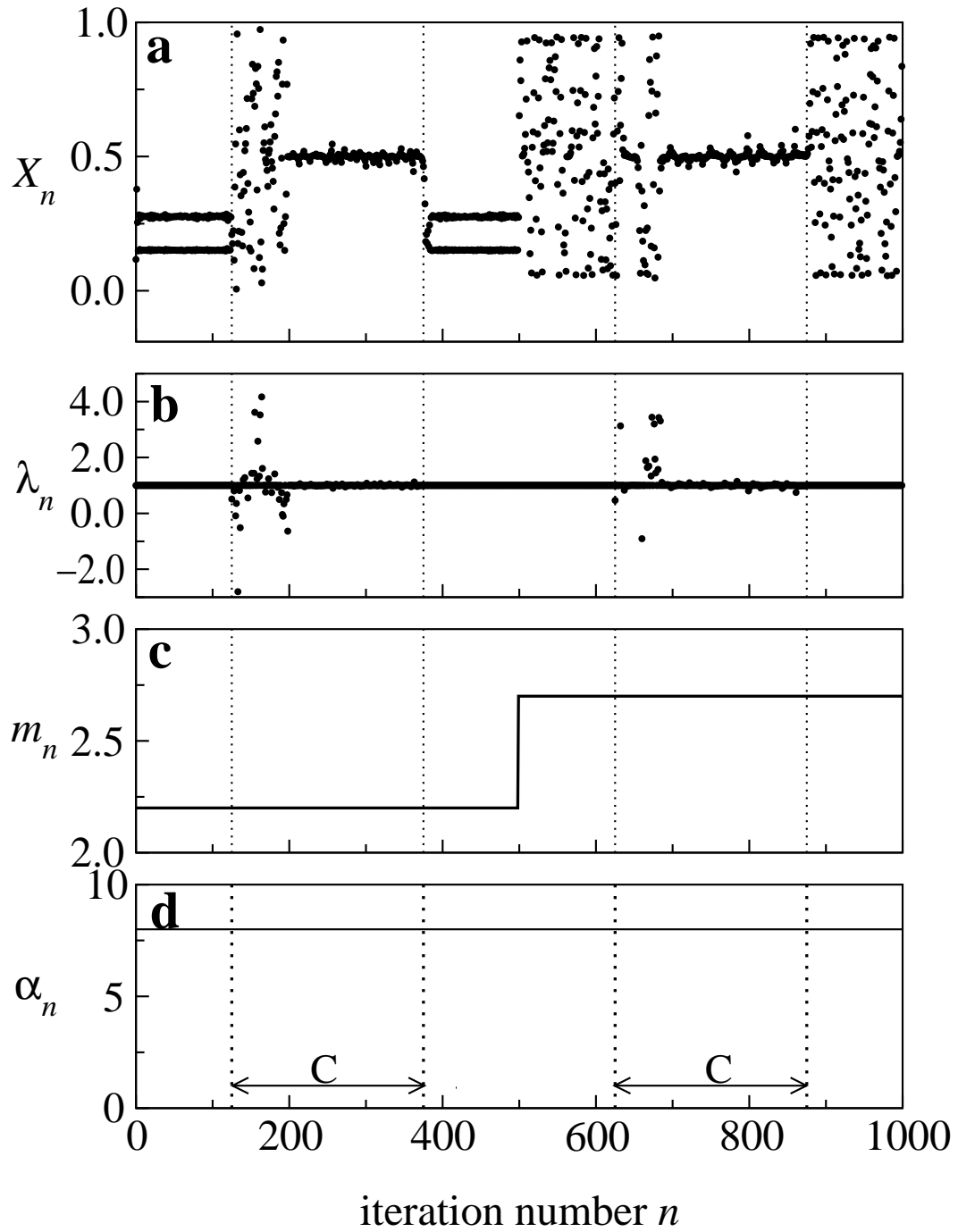


Fig. 8

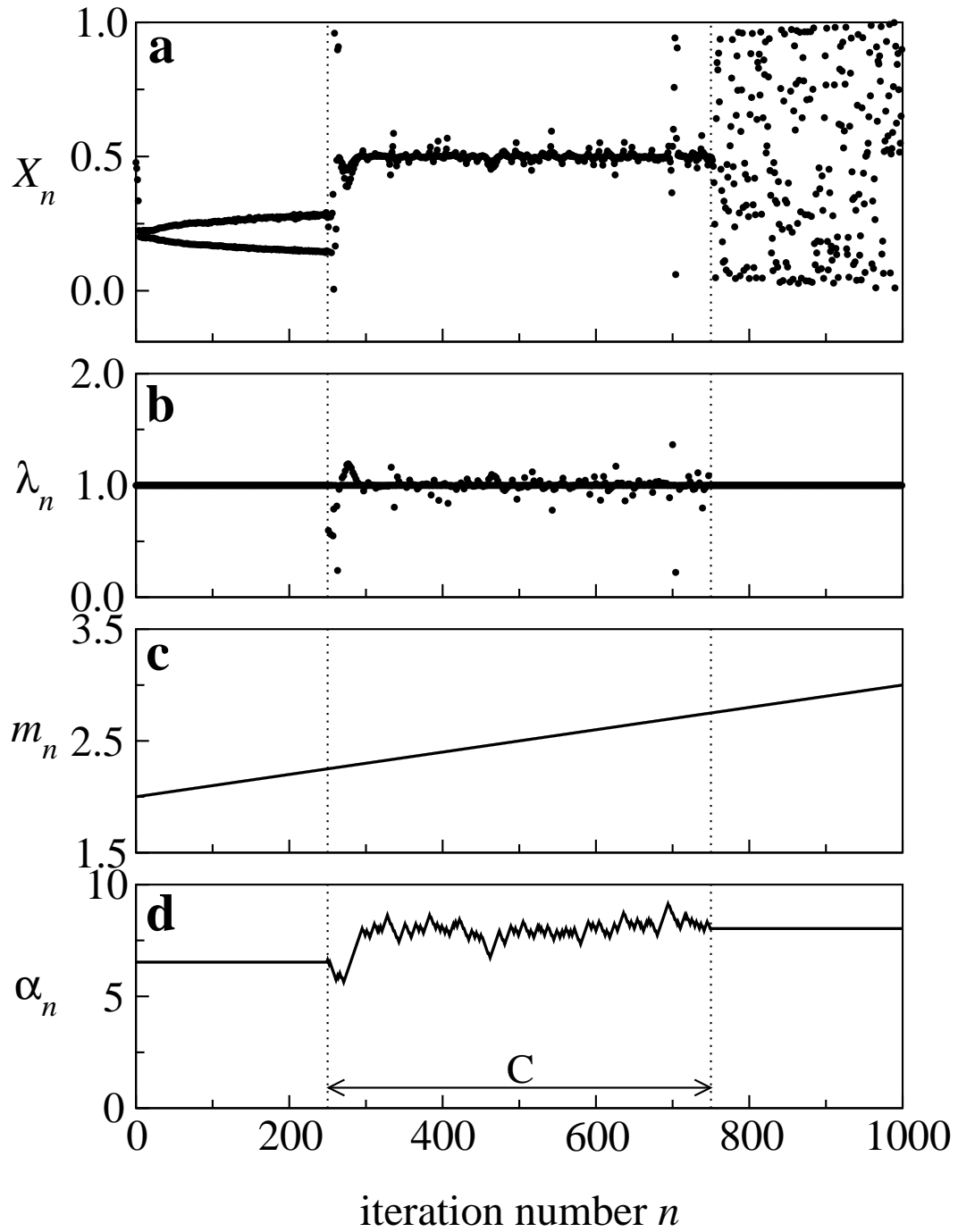


Fig. 9